African Journal of Pharmacy and Pharmacology Vol. 6(5), pp. 343-351, 8 February, 2012
Available online at http://www.academicjournals.org/AJPP
DOI: 10.5897/AJPP11.822
ISSN 1996-0816 © 2012 Academic Journals

Full Length Research Paper

A preliminary study on the evaluation of a novel gene delivery vector-TACS *in vitro* and *in vivo* via co-expressing hVEGF and hBMP genes to repair critical-size rabbit bone defects

Yu Wenyuan[1], Zhao Yu[1]*, Xing Yanli[1], Bai Xin[1], Fang Yuee[2], Zhang Lin[1], Ding Hao[1] and Wang Banghe[1]

[1]Department of Plastic Surgery, the First Affiliated Hospital, Anhui Medical University, Hefei 230032, P. R. China.
[2]Department of Polymer Science and Engineering, School of Chemistry and Materials Science, USTC, Hefei 230026, P. R. China.

Accepted 20 January, 2012

Strategies using gene therapy by nonviral vector to improve bone regeneration have been under research in the past. However, transfection efficiency into local cells, such as marrow stromal cells (MSCs) by each vector is not always high. Now, we fabricate a novel gene vector-thiolated N-Alkylated chitosan (TACS) by modifying of chitosan to overcome this problem. TACS is synthesized by conjugation of thiol group and alkyl group to the chitosan. Transfection efficiency of pcDNA3.1-EGFP into HEK293 with TACS increased significantly when compared with chitosan vector by the fluorescence microscope observation. As a next step, we constructed pIRES-hVEGF$_{121}$cDNA/hBMP-4 by using molecular cloning as a transfer gene to express angiogenic and osteogenic factor synergistically. Furthermore, using *in vivo* gene therapy, we evaluated the potential of TACS-pIRES-hVEGF$_{121}$CDNA/hBMP-4 as a novel strategy for the repair of critical-size rabbit bone defects *in vivo*. Strategy of TACS-pIRES-hVEGF$_{121}$cDNA/hBMP-4 gene therapy using TACS as a vector enhanced new bone formation significantly. These results suggest that TACS is a novel and potential gene vector and TACS-pIRES-hVEGF$_{121}$cDNA/hBMP-4 gene therapy is a feasible and simple effect tool for bone regeneration.

Key words: Gene therapy, nonviral vector, chitosan, vascular endothelial growth factor, BMP-4, bone tissue regeneration, tissue engineering.

INTRODUCTION

Fracture-healing repairment by autogenous or allogeneic bone transplantation faces a great limitation in clinical implications, due to lack of a graft source, immune rejection, significant cost and the inability to integrate with the surrounding host tissue. This area requires a simple and efficient method of treatment. The engineering of bone tissue which offers new therapeutic strategies to aid musculoskeletal healing is under research intensively by other authors (Meijer and de Bruijn, 2007). However, most strategies rely on progenitor cells, suitable scaffolds and morphogenetic stimuli to promote their differentiation into osteoblasts (Heinemann and Heinemann, 2009; Jo and Lee, 2007). This strategy may be effective, but requires operative interventions and substantial cost. Facilitated endogenous repair is a novel approach to tissue engineering that avoids the *ex vivo* culture of autologous cells and the need for manufactured scaffolds, while minimizing the number and invasiveness of associated clinical procedures. The strategy relies on harnessing the intrinsic regenerative potential of endogenous tissues using molecular stimuli, such as gene transfer, to initiate reparative processes *in situ* (Crombleholme, 2000; Fischer and Kolk, 2011).

*Corresponding author. E-mail: zhaoyu987654@gmail.com. Tel: +86-0551-2845009.

Gene transfer is a technology that delivers functionally active therapeutic genes into targeted cells. Osteogenic gene that was transferred to local cells may cause endogeneous targeted protein product to stimulate bone healing. Unlike proteins delivered exogenous, those synthesized endogenously will have authentic post-translational, modification and be free from the altered molecules that can reduce activity and provoke immune responses. Most importantly, it can be released at a sustain concentration which is essential for bone healing to induce an adequate osteoinductive stimulus (Andree and Kullmer, 2002; Bonadio, 2000; Evans and Palmer, 2007; Uusitalo and Hiltunen, 2001).

Gene transfer can be completed *in vivo* or *ex vivo*, and both approaches have been examined by animal experiments for bone regeneration (Bleiziffer and Eriksson, 2007). Yet, the complexity involved with cell isolation and culture emphasizes the advantages of direct gene delivery as an alternative strategy. During *in vivo* gene transfer, a vector carrying therapeutic DNA is directly implanted or injected into the patient, which is more likely to lead to a physiological tissue with fewer time and cost (Bleiziffer and Eriksson, 2007).

Transfer of gene for bone regeneration applications need appropriate vector. Although, many researchers use viral vector systems because their infection rates are relatively high, nonviral vector systems may be safer alternatives for gene therapy (Evans, 2010). They have potentialities to be administered repeatedly with minimal host immune response that are targetable, stable in storage and easy to produce in large quantities.

Chitosan is a potential promising nonviral vector, because of its natural and biocompatible composition. It is a biodegradable polysaccharide extracted from crustacean shells (Bozkir and Saka, 2004). It has been shown to effectively bind DNA in saline or acetic acid solution and protect DNA from nuclease degradation. Several transfection studies have reported both *in vivo* and *in vitro*, of a blemish which is limited *in vivo* efficacy. Now, we fabricate a novel gene vector-thiolated N-Alkylated chitosan, based on previous research that transfection efficiency is increased by the introduced alkyl side chains, and thiolated chitosan appears to possess enhanced mucoadhesiveness and cell penetration properties (Lai and Lin, 2009).

In this study, we reported firstly the prosperity of thiolated N-Alkylated chitosan (TACS) as a novel attractive gene vector and then gene transfection *in vitro* to suggest the transfection efficiency of TACS-pDNA nanoparticles; last use TACS delivery of osteogenic gene induce newbone formation *in vivo*.

For this study, we have successfully fabricated pIRES-hVEGF$_{121}$cDNA/hBMP-4 by using molecular cloning and gene transfection technique and expressed bone morphogenetic protein (BMP)/vascular endothelial growth factor (VEGF) successfully. BMPs play a critical role in the differentiation of osteoprogenitor cells and the bone formation process (Yoon and Boden, 2002). VEGF is an important angiogenesis cellular growth factor which is important during the bone healing process. It can improve the regeneration of capillary vessels and stimulate the initiation of vascularization and induce the synthesis of BMP (Deckers and van Bezooijen, 2002; Furumatsu and Shen, 2003). The synergistic interaction of BMP and VEGF has been reported both *in vivo* and *in vitro* (Peng and Wright, 2002; Samee and Kasugai, 2008). In the current study, we investigated the potentiality, feasibility strategy of direct gene transfect of pIRES-hVEGF$_{121}$cDNA/hBMP-4 with modify chitison vectors for repairing critical-size rabbit bone defects.

MATERIALS AND METHODS

In vitro studies

Construction of the recombinant coexpression plasmid pIRES-hVEGF$_{121}$/hBMP-4

The construction of the eukaryotic coexpression plasmid encoding VEGF and hBMP-4 has been previously described. Briefly, first, the plasmid pIRES and pGEM-Teasy-hVEGF$_{121}$ were digested with EcoRI. The IRES fragment was extracted with dehydrated alcohol, and the hVEGF$_{121}$ fragment was identified and extracted by 1% agarose gel electrophoresis. The acquired IRES fragment was dephosphorylated with shrimp alkaline phosphatase (SAP) then ligated with acquired hVEGF$_{121}$ fragment in the presence of T4 DNA ligase. Competent *Escherichia coli* DH10B were then transformed with the ligation mixture. Transformed bacteria were spread on Lysogeny broth (LB) agar plates and were incubated overnight at 37°C. Single clones were then picked and grown in LB medium supplemented with ampicillin. Plasmid DNA from individual clones was isolated using a vector Miniprep Kit. The acquired recombinant coexpression plasmid was identified and analyzed by digestion with restriction endonucleases (EcoR I and Nhe I). Secondly, pShuttle CMV-hBMP-4 was constructed by the same method, pcDNA3.1(+)-hBMP-4 and pShuttle CMV were digested with Xho I and Hind III, then identified, extracted and ligated as aforementioned. Finally, the construction of recombinant plasmid pShuttle CMV-hBMP-4 and pIRES-hVEGF$_{121}$ were digested with Xba I and Sal I, after which the fragments were identified, extracted and ligated. The positive clone was named pIRES-hVEGF$_{121}$cDNA/hBMP-4. We verified the reconstruction by combination of double digestion using Xba I and Sal I.

Cell culture and transduction

Mouse marrow stromal cells (MSCs) were isolated and cultured as previously described (Lee, 2000). These cells were harvested and washed with phosphate buffered saline (PBS) when at 80 to 90% confluence. The cells were resuspended in resuspension buffer R at a density of 1×10^7 cells/ml and incubated with 10 ul recombinant plasmid and 12 ul liposome, then placed at 37°C in a 5% CO_2 atmosphere. Transgene expression was detected at 48 and 72 h. The transduced cells were expanded for 2 weeks before being used in animal experiments.

BMP-4 and VEGF$_{121}$ mRNA detection western blotting

BMP-4 and VEGF$_{121}$ mRNA were detected in transfected cells by

Table 1. PCR amplifications performed using sense and antisense primers of BMP-4, $VEGF_{121}$ and angiopotein-1.

Gene	Sense primer (5'-3')	Antisense primer (5'-3')
BMP-4	GTACCATGATTCCTGGTAACCGAATGC	TCTAGATCAACGGCACCCACACCCTTCCACC
$VEGF_{121}$	GCTAGCATGAACTTTCTGCTGTCTTGG	GAATTCTCACCGCCTCGGCTTGTCACA
Angiopotein-1	GAGGGAAATCGTGCGTGAC	TAGGAGCCAGGGCAGTAATCT

reverse transcription-PCR (RT-PCR). Total cellular RNA was isolated from harvested cells at 72 h after transduction using Trizol reagent. Extracted RNA was treated with DNase I to eliminate DNA contamination and first-strand cDNA was synthesized by random hexamer. The PCR amplifications were performed using sense and antisense primers of BMP-4 and $VEGF_{121}$ and angiopotein-1 as listed in Table 1. Angiopotein-1 was detected by RT-PCR as an internal control. The RT-PCR was performed by using the AccessQuick™ RT-PCR kit. The products were analyzed using 1.2% agarose gel electrophoresis.

48 h after transfection, cells were washed twice in ice-cold PBS and then lysed with 200 ul lysis buffer to obtain total cellular protein. Supernatants were analyzed by western blotting after centrifugation (20000 g for 5 min). Equal amounts of cell extracts were separated in a sodium dodecyl sulfate polyacrylamide gel electrophoresis (SDS-PAGE) (100 V, 2 h). After electrophoresis, fractioned proteins were transferred from the gel to a polyvinylidene difluoride membrane and were blocked in 5% (wt/vol) skim milk in tris-buffered saline tween-20 (TBST) for 2 h at 4°C. Subsequently, the membrane was incubated with primary mouse-anti-human BMP antibody (1:250 dilution) for 2 h at room temperature. After washing in PBS thoroughly, the membrane was incubated with secondary sheep anti-mouse antibody (1:40000) for 1 h at room temperature. The immunoreactive bands on the membrane were detected by using ECL Western Blotting Detecting Kit.

The construction of TACS vector and the preparation of chitosan-DNA nanoparticles

TACS is synthesized by conjugation of thiol group and alkyl group to the chitosan. First, N-Alkylated chitosan (CS) was synthesize by the traditional method which has been reported in previous study (Yang and Chou, 2002). Briefly, 1 g of CS was added into 40 ml of 15 ml isopropanol/2.5 g sodium hydroxide solution and was stirred at 70°C for 30 min. The dodecyl bromide was added dropwise to the mixture and allowed to react for 6 h, and then, the reaction mixture was centrifuged. The obtained precipitate was washed with ethanol and then dried at vacuum to obtain the 12-alkylated chitosan derivatives (12-CS). The resultant alkylated chitosan derivatives were dialyzed for 3 days using Cellu SepH1 membrane (MWCO 12000) against water. The degree of substitution was determined by traditional potentiometric titration. Second,12-CS of 0.5 g was dissolved in 50 ml of hydrochloric acid solution (1.0%) to which 0.5 g thioglycolic acid (TGA) was added (Kast and Frick, 2003). In order to activate the carboxylic acid moieties of TGA, 200 M of 1-ethyl-3-(3-trimethy laminopropyl) carbodiimide hydrochloride (EDAC) was added. The pH of the solution was adjusted from 4.5 to 5.0 using 1 M NaOH and the chemical reaction was allowed to run at room temperature protection from light for 3 h. To eliminate unbound TGA and isolate the conjugated polymers, the reaction mixture was dialyzed using hydrochloric acid solution(1 mM) for 12 h, then hydrochloric acid solution (1 mM) (include 1% NaCl) for 1 day. The chitosan conjugate was lyophilized at -30°C and was stored at 4°C until further use. The degree of thiol groups of the 12-CS-thioglycolic acid conjugate was determined at room temperature using Ellman reagent.

The TACS/pDNA nanoparticles were prepared by complex coacervation of TACS and pIRES-h$VEGF_{121}$cDNA/hBMP-4 as shown previously. TACS was dissolved in 5 mM sodium acetate buffer (pH 5.5) to form a solution of 1 mg/ml. DNA solution was dissolved in 50 mM Na_2SO_4 solution to form a solution of 76 ug/ml. Chitosan/DNA complexes were prepared by mixing chitosan solution with DNA solution, vortexed for 15 s and incubated for 30 min at room temperature. Particle size and zeta potential of chitosan/pDNA nanocomplexes were measured using a Zetasizer Nano ZS-90 (Malvern Co., Ltd., USA) at 25°C.

Transfection efficiency and cell viability effect of TACS

The TACS/pcDNA3.1-EGFP nanoparticles were prepared by complex coacervation method, as mentioned earlier. Using a report gene, pEGFP, CH-RGD'pEGFP nano-gene transfer system was compared to CH-pEGFP nano-gene transfer system and another polycationic polymer, lipofetamine 2000, in the transfection efficiency with Hy926 cells *in vitro*.

In vivo bone formation

Fifteen white New Zealand rabbits weighing 2.0 to 3.0 kg each were used in this study and 30 legs divided into two groups (left leg of each as experimental group, right leg of each as control group). Each group of rabbits had undergone operations to assign a bone defect of 15 mm in the middle of the radii in 15 (30 sides). After excise, the periosteum of the normal bone around the defect, then implanted the gelatin sponge into the fracture site (1 × 1 × 1 cm). Left Legs in experimental group received intro-injections of chitosan-DNA nanoparticles 0.5 ml (25 ug/ml) (n = 15), right legs in control group received an injection of the same volume of physiologic saline (n = 15). Chitosan-DNA nanoparticles solutions which were stored at 4°C were injected into the gelatin sponge which was implanted into the bone defect site using microinjector. The gelatin sponge was used as a carrier which could strengthen the local osteogenetic induction effect, because of its porous structure, good biocompatibility and biodegradable performance. All the animal experiments were approved by the animal Research and Care Committee of the Anhui Medical University.

X-rays and determination of radiopacity density: At 6/8/12

weeks postsurgery, anteroposterior and lateral X-rays of the radius were obtained for all rabbits, while they were under general anesthesia to determine the features of regeneration, using standardized tube to leg distance, kilovolts (0 kV) and milliamps (100 mAs), 0.97 s each time. Features examined included the amount of the callus formed, osseous bridging of the gap and corticalization of the regenerated bone (Figure 5). To detect the radiopacity density of new bone in detect area, we normalize the radiopacity density of os integumentale in the same area as 100 for

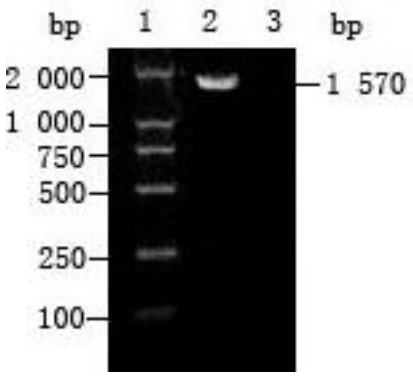

Figure 1. Detection of BMP4 mRNA in mBMSC by RT-PCR. Lane 1, Marker; lane 2, BMP4 amplification of mBMSC/pIRES-BMP2-VEGF$_{165}$; lane 3, negative control group.

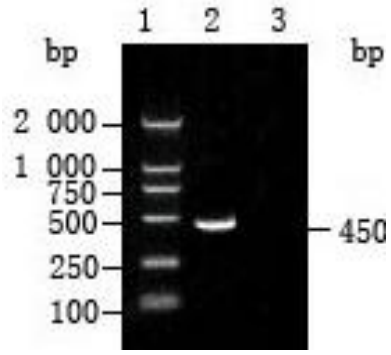

Figure 2. Detection of VEGF$_{121}$ mRNA in mBMSC by RT-PCR. Lane 1, marker; Lane 2, VEGF$_{165}$ amplification of mBMSC/pIRES-BMP2- VEGF$_{165}$; Lane 3, negative control group.

positive control, and negative control normalizes as 0.

Immunohistochemical and histological analysis: At 6/8/12 weeks postsurgery, animals were euthanized and their fracture healing specimens were collected (n = 5). The specimens from each group at each time were analysized. For immunohistochemical, according to conventional streptavidin-perosidase protocol, the first antibodies were rabbit monoclonal antibodies against human BMP-4, color developing reagent was diaminobenzidine (DAB) (Figure 7).

For histology, specimens were fixed in 10% buffered pormalin and embedded in paraffin. Serial transverse and longitudinal sections (5 μm) were prepared and stained with hematoxylin and eosin (H&E). Percent trabecular area (%Tb.Ar) for each section was determined by dividing the total number of pixels for the total trabecula area percentage using Photoshop 6.0 software (take five high-powered fields of each section). Three sections per animal were analyzed in a blinded fashion, and the mean of these three sections was used for statistical analysis.

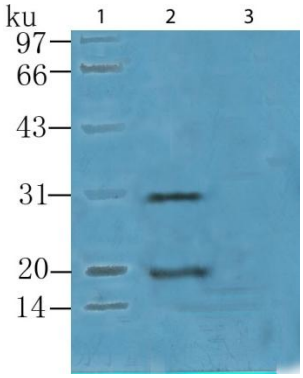

Figure 3. Co-expression of BMP2 and VEGF$_{165}$ proteins in mBMSC detected by western blot. Lane 1, marker; lane 2, BMP2 and VEGF$_{121}$ protein detection of mBMSC/pIRES-BMP2-VEGF$_{165}$; lane 3, negative control group.

Statistical analysis

All values, expressed as means + standard error (SE), were subjected to t test and one-way analysis of variance (ANOVA) employing the computer SPSS 13.10 statistic package. A P-value of <0.05 was considered statistically significant.

RESULTS

Expression of BMP-4 and VEGF$_{121}$ gene and protein production by transduction *in vitro* RT-PCR generated 1570 and 450 bp products in pIRES-BMP-4-VEGF$_{121}$ transfected samples. Cells nontransfected produced no RT-PCR products (Figures 1 and 2). Western blot generated 32 and 20 ku products in MSCs transfected with pIRES-BMP-4-VEGF$_{121}$ vector, however, the control cells were negative (Figure 3). The results suggest that mBMSC transfected with pIRES-BMP-4-VEGF$_{121}$ vector can coexpress mRNA and the proteins of BMP-4 and VEGF$_{121}$.

In vivo bone formation

The conditions included the blank group (no factors only the gelatin sponge and physiologic saline 0.5 ml) and experimental group (the gelatin sponge and chitosan-DNA nanoparticles 0.5 ml). X-ray and histological analysis of explants at 6/8/12 weeks revealed new bone formation in blank group and experimental group (Figure 6). 2 days postsurgery, forelimb of rabbits cannot load on the ground. 1 week later, they can resume normal activities. Surgical incision was healing without swelling and exudates.

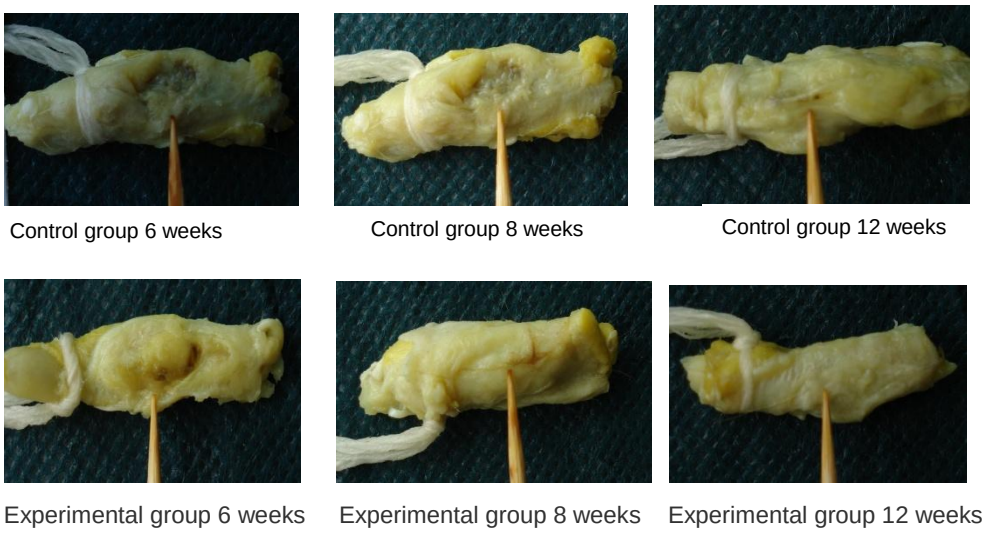

Figure 4. The experimental group (left radial bone) and the control group (right radial) 6, 8 and 12 weeks general observation (nitric acid decalcified samples).

Table 2. X-ray analysis of bone defect density of the average fire resistance (P < 0.05).

Group	6 weeks	8 weeks	12 weeks
Experimental *	48.12 ± 1.25	64.14 ± 1.21	79.16 ± 1.25
Control*	32.87 ± 1.19	38.21 ± 1.51	39.22 ± 3.79

*. P < 0.05; the repairing capability and rate of osteogenesis in experiment group were significantly higher than those in control group (P < 0.01).

Macroscopic examination of the bone defect area

1. 6 weeks postsurgery: Significant callus formation can be observed at the area of bone defects of the experimental group. Defect sites were filled with bone-like tissue with certain intensity, while fibrous connective tissue was found on the peripheral package of the control group.
2. 8 weeks postsurgery; the formation of new bone tissue of the experimental group was significantly higher than the control group.
3. 12 weeks postsurgery; the bone defect site of experimental group has a harder and more obvious bone formation. The defects were restored mainly. While there is a obvious depression at the bone defect of the control group (Figure 4).

X-rays observations and determination of density radiopacity

Osseous images were found in the experimental areas by X-ray examination at 6 weeks after injection with bony callus of cloudy and continuous distribution in bone defects (Figure 5). On the contrary, no osseous images were observed on the control sides. Only little bony callus can be observed at the end of the defected bone with only a small number of cloudy callus formation. 8 weeks after surgery, bony union was consecutive and small strips of bone could be found in the experimental group when compared with the control group which showed the distribution of callus only at the end of the defect. Furthermore, the callus density was lower than that in the experimental group. At 12 weeks, in the experimental group, it was found that the bony callus was consecutive evenly distributed throughout the bone defect and Medullary cavity recanalization defect was completely repaired, while the control group only found callus formation at both end of the defects, the central part of the defect had no significant bone formation images (Figure 5). The two groups at different time X-ray bone defect density radiopacity are as shown in Table 2.

Histological evaluation of the new bone

Examination of sections stained with H&E supported the results of X-ray imaging, because only a small bone formation was observed in H&E-stained sections in the control group. These conditions led only to fibrous tissue

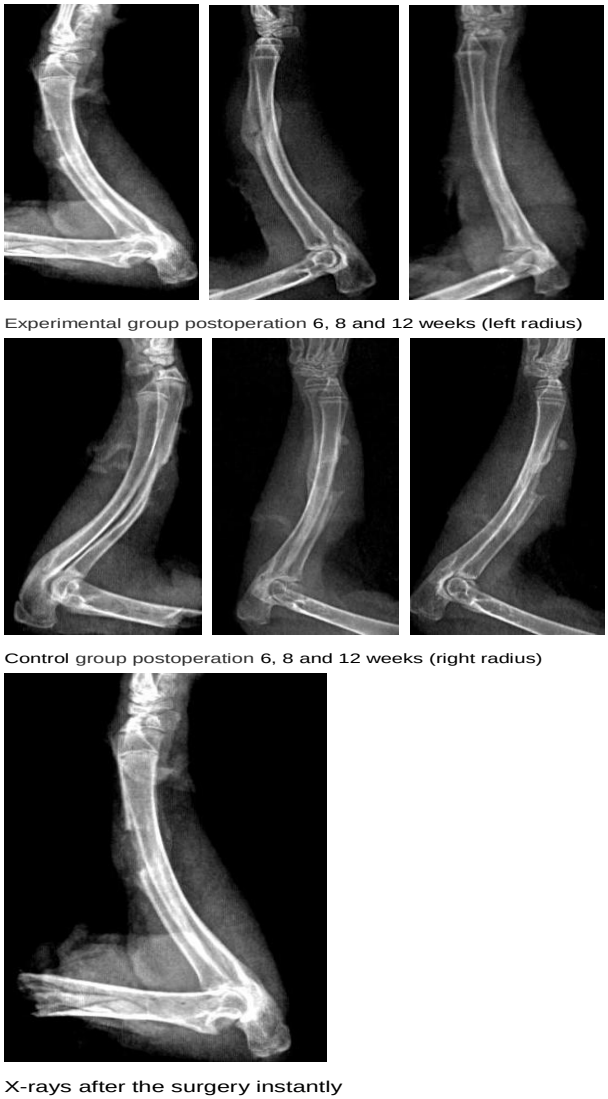

Figure 5. Experimental group, control group at 6, 8 and 12 weeks X-ray and after the surgery instantly findings

Table 3. The new trabecular bone defect accounted for the percentage size of the area.

Group	6 weeks	8 weeks	12 weeks
Experimental	38.87 ± 0.25	72.53 ± 0.42	96.87 ± 0.35
Control	21.38 ± 0.22	28.73 ± 0.38	32.33 ± 0.37

ingrowths and the formation of small spicules of bone on the peripheral region of the blank. In contrast, delivery of a combination of BMP and VEGF via TACS, in the bony tissue development with a resemblance of the immature woven bone formation full of blood vessels was observed at 8 weeks, whereas interconnected bone trabeculae were visible at 12 weeks with large amounts of mature lamellar bone bridge that can be seen in the medullary cavity recanalization. The formation of osteoid can be seen with a large number of active proliferations of osteoblasts and cartilage cells and angiogenesis at 6 weeks. Moreover, the percent trabecular area measurement 6,8 and 12 weeks postoperatively at the sites of bone defects revealed that the results of the experimental group were significantly higher than their controls ($P < 0.05$) (Table 3 and Figure 6).

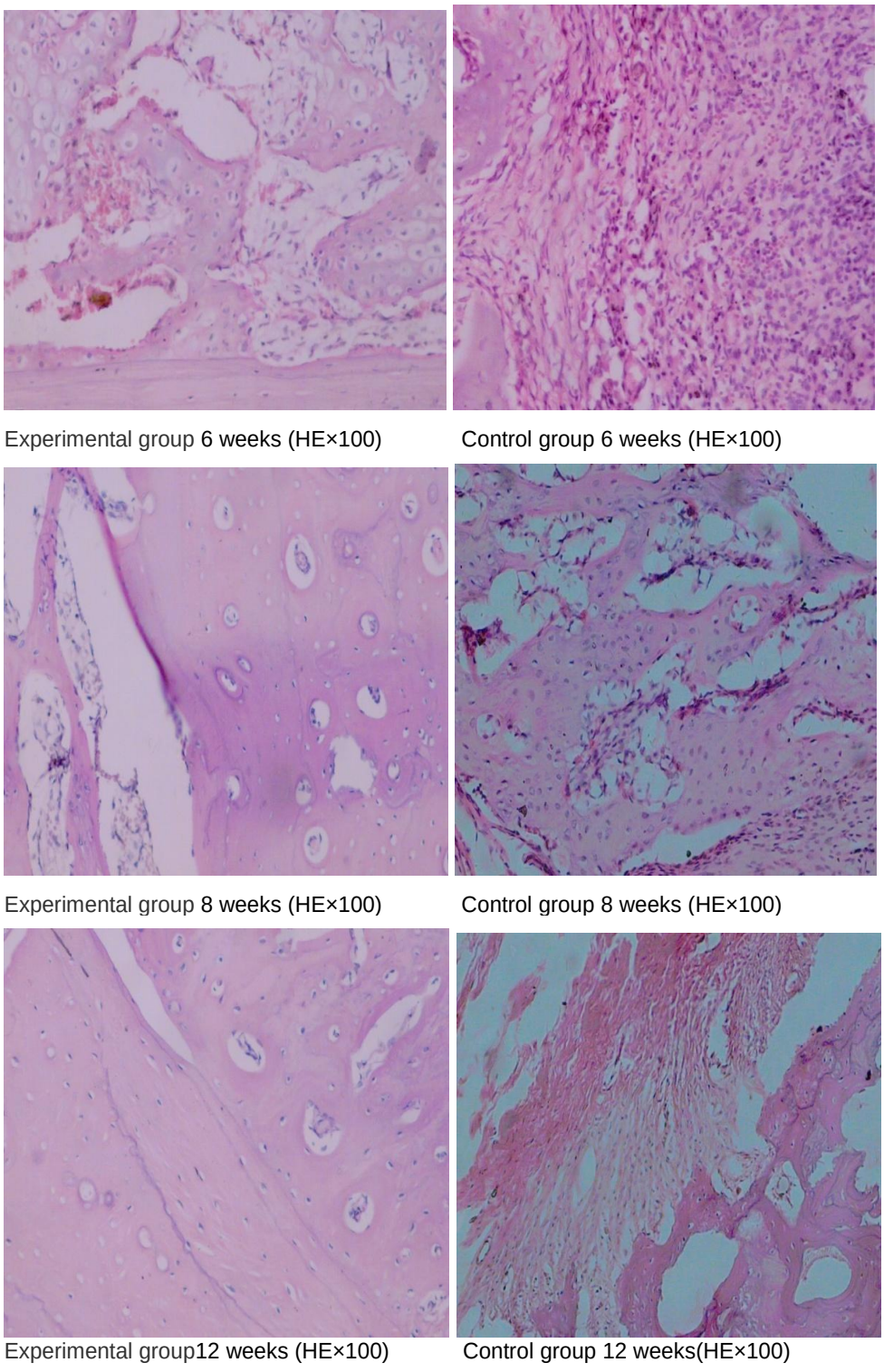

Figure 6. The experimental group and control group, 6, 8 and 12 weeks histological.

Immunohistochemical detection of BMP-4 expression

Immunohistochemical analysis confirmed that BMP-4 observed display in experimental group at 6 weeks. The expression of BMP-4 was strong positive as these dark tan particles were found around the new bone matrix and bone trabecular, while the blank group with little tan particles reveals a weak or no expression of BMP-4

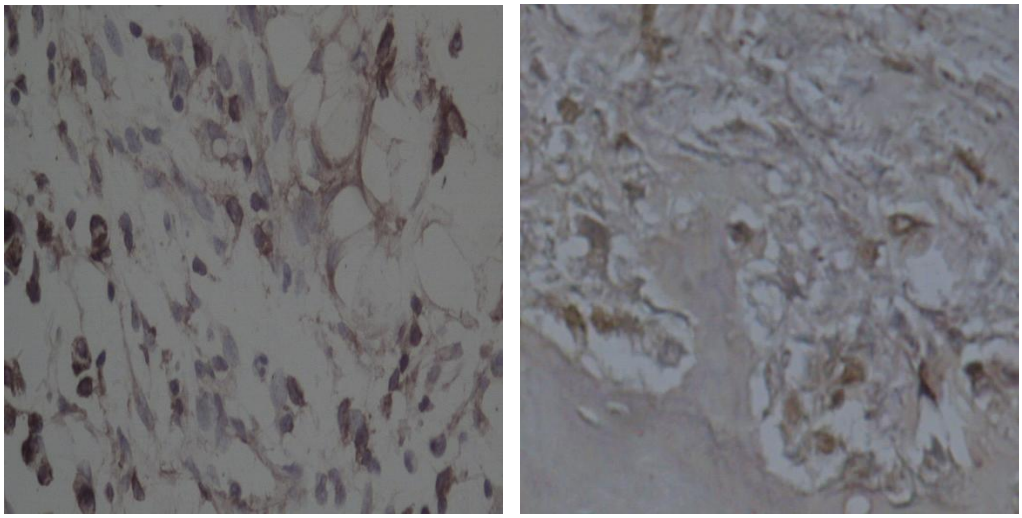

Experimental group 6 weeks (×400) Control group 6 weeks (×400)

Figure 7. The experimental group and control group 6 weeks immunohistochemical detection of BMP-4 expression.

(Figure 7).

DISSCUSSION

Natural bone regeneration is a highly coordinated process. In this process, various factors were involved and interacted with each other to promote bone regeneration significantly. BMPs molecules initiating vascularization (e.g. vascular endothelial growth factor [VEGF]) are the most important factors which promote recruitment of mesenchymal cells to bone formation and regenerate sites and enhances cell survival (Yoon and Boden, 2002). In the present study, critical-sized segmental defects in rabbit radii were repaired by co-expression of BMP-4 and $VEGF_{121}$ via *in vivo* gene therapy by a novel gene vector-thiolated N-Alkylated chitosan (TACS). A previous study showed that dual delivery of the two growth factors (BMPs and VEGF) led to the greatest quantity and highest quality of new bone tissue compared with each factor alone, indicating that BMPs and VEGF acted together to regenerate bone tissue (Xiao and Zhou, 2011). We successfully fabricated recombinant plasmid vector co-expression of BMP-4 and $VEGF_{121}$ gene, and detect the BMP-4 and $VEGF_{121}$ proteins co-expression in the transfected MSCs of pIRES-hBMP4-hVEGF$_{121}$ by adeno-virus vector. The vector system developed for this study is based on chitosan, a widely used nonviral vector that has been safely used to bind DNA by complex coacervation and protect it from nuclease degradation and transfect to cells of a blemish which is limited in transfection efficacy (Dastan and Turan, 2004; Saranya and Moorthi, 2011; Sato, 2009). By the introduction of alkyl side chains and thiolated chains to chitosan, we fabricated a novel nonviral vector-TACS (thiolated N-Alkylated chitosan) which appears to possess enhanced mucoadhesiveness and cell penetration properties and have an increased transfection efficiency most of all (Kurita and Mori, 2002; Ma and Yang, 2008; Martien and Loretz, 2007; Schmitz and Bravo-Osuna, 2007). By the injection of TACS-pIRES-hVEGF$_{121}$cDNA/hBMP-4, critical-sized segmental defects in rabbit radii were repaired compared with the control group. Proteins, such as VEGF and BMP can be readily expressed, allowing for a sustained and localized release at an implant site of a bioactive form of the growth factor (Ma and Yang, 2008). But the impact of condensation of plasmid DNA on the bone defect regeneration was still unclear, and the effect of the coexpression and sustained presentation of osteogenic and angiogenic growth factors via a nonviral vector was first reported in a genetic engineering approach.

Plasmid DNA potentially can be taken up by infiltrating surrounding host cells (e.g. fibroblasts, BMSCs). The BMP-4 secreted by both cell sources likely acted in both autocrine and paracrine manners by directly differentiating the hBMSCs into osteoblasts and initiating the differentiation of osteoprogenitors from the host tissue into bone-forming cells. BMP-4 could also have served as an osteoinductive signal to increase infiltration and recruitment of surrounding repair cells to further enhance bone regeneration. BMP-4 expression was examined at 6 weeks postsurgery by immunohistochemical detection and was used to verify the experimental group that has a high expression of BMP4. Several mechanisms may underlie a direct or indirect role of VEGF in bone formation in these studies. VEGF is essential for endochondral bone formation (Bozkir and Saka, 2004),

and this may be related to its ability to induce migration (Samee and Kasugai, 2008) and differentiation of osteoblasts (Saranya and Moorthi, 2011). VEGF-induced angiogenesis may also increase the migration and differentiation of bone marrow stromal cells, because of both increased nutrient availability and signaling interactions between endothelial cells and hBMSCs (Sato, 2009). For example, treatment of endothelial cells with VEGF *in vitro* has been shown to result in enhanced expression of BMP-2, another osteogenic growth factor capable of inducing differentiation of osteoblasts (Schmitz and Bravo-Osuna, 2007; Uusitalo and Hiltunen, 2001). Although, bone formation was more significant in delivering both VEGF and BMP-4 by TACS than control group, it is only an initial research of the co-expression gene plasmid vector and the novel vector of verified chitosan. Both theories deserve further investigation.

Qualitative observation of X-rays images indicated a more rapid formation of bony tissue and more highly interconnected bony trabeculae in the condition delivering BMP-4, VEGF and TACS than the black condition. Whereas, the moduli of the other conditions were two to three orders of magnitude lower than that seen in normal trabecular bone (50 to 100 Mpa), the moduli of scaffolds delivering BMP-4, VEGF and hBMSCs were only approximately one order of magnitude lower than normal trabecular bone. The greater moduli observed in this condition are likely related to the increased bone volume in these tissues, thicker bony trabeculae and increased interconnectivity of the bone microarchitecture. Altogether, these data indicated that the quality of new bone formed in scaffolds with the three factors combined was superior both structurally and mechanically to other conditions.

In summary, this study shows the *in vivo* gene therapy, the prosperity of TACS as a novel attractive gene vector transfer osteogenic and vascugenic co-expression gene to host cells to induce newbone formation. This combined novel therapy used TACS and a gene vector may find therapeutic applications. But the transfection efficiency of TACS as a nonviral vector *in vivo* needs a deep research.

REFERENCES

Andree C, Kullmer M (2002). Gene technology and tissue engineering. Mini. Invasive Ther., 11(3): 93-99.

Bleiziffer O, Eriksson E (2007). Gene transfer strategies in tissue engineering. J. Cell Mol. Med., 11(2): 206-223.

Bonadio J (2000). Tissue engineering via local gene delivery. J. Mol. Med., 78(6): 303-311.

Bozkir A, Saka OM (2004). Chitosan nanoparticles for plasmid DNA delivery: Effect of chitosan molecular structure on formulation and release characteristics. Drug Deliv., 11(2): 107-112.

Crombleholme TM (2000). Adenoviral-mediated gene transfer in wound healing. Wound Repair Regen., 8(6): 460-472.

Dastan T, Turan K (2004). In vitro characterization and delivery of chitosan-DNA microparticles into mammalian cells. J. Pharm. Pharm. Sci., 7(2): 205-214.

Deckers MML, van Bezooijen RL (2002). Bone morphogenetic proteins stimulate angiogenesis through osteoblast-derived vascular endothelial growth factor A. Endocrinology, 143(4): 1545-1553.

Evans CH (2010). Gene therapy for bone healing. Expert Rev. Mol. Med., pp. 12-10.

Evans CH, Palmer GD (2007). Facilitated endogenous repair: making tissue engineering simple, practical, and economical. Tissue Eng. Part A, 13(8): 1987-1993.

Fischer A, Kolk (2011). Future of local bone regeneration - Protein versus gene therapy. J. Cranio-Maxillofac. Surg., 39(1): 54-64.

Furumatsu ZN, Shen (2003). Vascular endothelial growth factor principally acts as the main angiogenic factor in the early stage of human osteoblastogenesis. J. Biochem., 133(5): 633-639.

Heinemann C, Heinemann S (2009). In itro Evaluation of Textile Chitosan Scaffolds for Tissue Engineering using Human Bone Marrow Stromal Cells. Biomacromolecules. 10(5): 1305-1310. Jo I, Lee JM (2007). Bone tissue engineering using marrow stromal cells. Biotechnol. Bioproc. E., 12(1): 48-53.

Kast CE, Frick W (2003). Chitosan-thioglycolic acid conjugate: a new scaffold material for tissue engineering. Int. J. Pharmaceut., 256(1-2): 183-189.

Kurita K, Mori S (2002). N-Alkylation of chitin and some characteristics of the novel derivatives. Polym. Bull., 48(2): 159-166.

Lai WF, Lin MCM (2009). Nucleic acid delivery with chitosan and its derivatives. J. Control Release, 134(3): 158-168.

Lee JY (2000). Clonal isolation of muscle-derived cells capable of enhancing muscle regeneration and bone healing. J. Cell. Biol., 150: 1085-1100.

Ma GP, Yang DZ (2008). Preparation and characterization of N-alkylated chitosan derivatives. J. Appl. Polym. Sci., 109(2): 1093-1098.

Martien R, Loretz B (2007). Chitosan-thioglycolic acid conjugate: An alternative carrier for oral nonviral gene delivery. J. Biomed. Mater. Res. A., 82A(1): 1-9.

Meijer GJ, de Bruijn JD (2007). Cell-based bone tissue engineering. PLos. Med., 4(2): e9.

Peng HR, Wright V (2002). Synergistic enhancement of bone formation and healing by stem cell-expressed VEGF and bone morphogenetic protein-4. J. Clin. Invest., 110(6): 751-759.

Samee M, Kasugai S (2008). Bone morphogenetic protein-2 (BMP-2) and vascular endothelial growth factor (VEGF) transfection to human periosteal cells enhances osteoblast differentiation and bone formation. J. Pharm. Sci., 108(1): 18-31.

Saranya N, Moorthi A (2011). Chitosan and its derivatives for gene delivery. Int. J. Biol. Macromol., 48(2): 234-238.

Sato T (2009). Gene Delivery System Using Chitosan Nanoparticles. J. Gene. Med., 11(12): 1142-1142.

Schmitz T, Bravo-Osuna I (2007). Development and in vitro evaluation of a thiomer-based nanoparticulate gene delivery system. Biomaterials, 28(3): 524-531.

Uusitalo H, Hiltunen A (2001). Induction of periosteal callus formation by bone morphogenetic protein-2 employing adenovirus-mediated gene delivery. Martix Biol., 20(2): 123-127.

Xiao C, Zhou H (2011). Bone marrow stromal cells with a combined expression of BMP-2 and VEGF-165 enhanced bone regeneration. Biomed. Mater., 6(1): 015013.

Yang TC, Chou CC (2002). Preparation, water solubility and rheological property of the N-alkylated mono or disaccharide chitosan derivatives. Food Res. Int., 35(8): 707-713.

Yoon ST, Boden SD (2002). Osteoinductive molecules in orthopaedics: Basic science and preclinical studies. Clin. Orthop. Relat. R., 39(5): 33-43.